Greenland Ice Sheet Mass Balance Reconstruction. Part III: Marine Ice Loss and Total Mass Balance (1840–2010)

JASON E. BOX*

Byrd Polar Research Center, The Ohio State University, Columbus, Ohio

WILLIAM COLGAN

Geological Survey of Denmark and Greenland (GEUS), Copenhagen, Denmark, and Cooperative Institute for Research in Environmental Sciences, Boulder, Colorado

(Manuscript received 31 July 2012, in final form 4 March 2013)

ABSTRACT

Greenland ice sheet mass loss to the marine environment occurs by some combination of iceberg calving and underwater melting (referred to here as *marine ice loss*, L_M). This study quantifies the relation between L_M and meltwater runoff (R) at the ice sheet scale. A theoretical basis is presented explaining how variability in R can be expected to govern much of the L_M variability over annual to decadal time scales. It is found that R enhances L_M through three processes: 1) increased glacier discharge by ice warming–softening and basal lubrication–sliding; 2) increased calving susceptibility through undercutting glacier front geometry and reducing ice integrity; and 3) increased underwater melting from forcing marine convection. Applying a semi-empirical $L_M f(R)$ parameterization to a surface mass balance reconstruction enables total ice sheet mass budget closure over the 1840–2010 period. The estimated cumulative 171-yr net ice sheet sea level contribution is 25 ± 10 mm, the rise punctuated by periods of ice sheet net mass gain (sea level drawdown) (1893–1900, 1938–47, and 1972–98). The sea level contribution accelerated at 27.6 mm yr^{-1} century^{-1} over the entire reconstruction, reaching a peak sea level rise contribution of 6.1 mm decade^{-1} during 2002–10.

1. Introduction

Ice sheet mass balance exerts a significant influence on global mean sea level (e.g., Huybrechts et al. 2004; Church and White 2011), thermohaline circulation (e.g., Fichefet et al. 2003; Rahmstorf et al. 2005), and ocean sediment nutrient influx (Rysgaard et al. 2003; Hasholt et al. 2006). A likely global sea level rise of 1 m or more by the century's end (e.g., Pfeffer et al. 2008) will come at massive infrastructural and livelihood costs.

Ice flowing into the marine environment around Greenland is removed from the ice sheet through a combination of iceberg calving (e.g., Benn et al. 2007; Howat et al. 2010) and underwater melting (Motyka et al. 2003; Rignot et al. 2010; Xu et al. 2012). Underwater melting can undercut glacier front geometry and increase iceberg calving susceptibility. Iceberg calving affects the force balance at glacier fronts. Thomas (2004) and Joughin et al. (2008) demonstrate that the stability of tidewater glacier fronts is a dominant control of upstream, inland, flow speed, and glacier ice discharge to the marine environment. Calving directly reduces the back-stress opposing glacier flow, leading to immediate flow acceleration. Back-stress resistance at the lateral margins, and potentially at the bed, may rebuild as the calving front advances. At Jakobshavn Isbrae, van der Veen et al. (2011) suggest that changes in resistive stress at the lateral shear margins may dominate changes in flow speed through reduced ice viscosity due to cryo-hydrologic warming driven by enhanced meltwater availability (Phillips et al. 2010, 2013). Surface meltwater also contributes to enhanced basal sliding through local lubrication and pressurization of the subglacial water drainage network (Zwally et al. 2002). Thus, surface meltwater plays a multifaceted role in enhancing both ice flow into the marine environment and underwater

* Current affiliation: Geological Society of Denmark and Greenland, Copenhagen, Denmark.

Corresponding author address: Jason E. Box, Geological Survey of Denmark and Greenland, Øster Voldgade 10, DK-1350 Copenhagen, Denmark.
E-mail: jeb@geus.dk

DOI: 10.1175/JCLI-D-12-00546.1

melting that is independent of variability in distant ocean currents (Holland et al. 2008).

Here, iceberg calving and underwater melting processes are combined into a single parameter termed marine ice loss (L_M). A semiempirical parameterization of L_M as a function of runoff (R) enables total ice sheet mass budget closure. Rignot et al. (2008) parameterized L_M in terms of a linear function of surface mass balance (SMB). Here, that relation is revisited using updated L_M data beginning in 1992 (Rignot et al. 2011). Surface mass balance and runoff data are after Box et al. (2006, 2009) and Part II of this series (Box 2013, hereafter Part II) spanning 171 years (1840–2010). Both R and SMB data are smoothed over a range of temporal intervals, from 1 to 17 years, to assess the time scale of peak sensitivity, or correlation, with L_M. Polynomial fits between L_M and SMB or R of order 1 through 3 are considered for the potential parameterization of whole ice sheet marine ice loss from a given surface mass balance or runoff. Finally, a physical basis is suggested in context of a theory for whole ice sheet marine ice loss varying with surface melting.

2. Data

a. Whole ice sheet marine ice loss

Twenty annual L_M estimates in the 1958–2009 period were obtained for this study from E. Rignot (2011, personal communication). These data were calculated from the ''flux gate'' method (Rignot and Kanagaratnam 2006), which determined horizontal ice velocity in the 1992–2009 period from satellite radar interferometry and ice sounding radar-derived ice thickness profiles normal to ice flow. The 1958 and 1964 estimates are based on extrapolation from a subset of 19 west Greenland glaciers and relatively short (less than 2 week) time interval repeat air photos (Bauer et al. 1968; Carbonnell and Bauer 1968). Surface mass balance calculations after Box et al. (2006) and Hanna et al. (2008) are used to estimate ice loss due to surface melting in the area below the flux gate. The L_M data after Rignot et al. (2008) from 1958 and 1964 have an assumed uncertainty of 20% or 103 Gt yr^{-1}. The L_M data after Rignot et al. (2011) from 1992 to 2009 have an estimated uncertainty of 5.5% or 31 Gt yr^{-1}, which accounts for uncertainties in ice thickness, thinning rate, velocity, and surface mass balance.

b. Surface mass balance

A continuous 171-yr annual surface mass balance and runoff reconstruction (1840–2010) are available to this study from Part II. This reconstruction was based on a spatial and temporal statistical assimilation of meteorological station records, ice cores, and regional climate model output.

Ice core observations and Regional Atmospheric Climate Model version 2 (RACMO2) solid precipitation output were combined to develop a time-varying spatial reconstruction of the Greenland ice sheet net snow accumulation rate spanning 410 yr (1600–2009). (See Part I of this series; Box et al. 2012, hereafter Part I). Rates of water vapor transfer between the surface and atmosphere are implicitly contained within the net ice core accumulation data that calibrate and drive the reconstructed accumulation rates.

Meltwater production was computed from the sum of surface air temperatures above the melting point and positive degree-day (PDD) factors for snow (DDF_{Snow}) and bare ice (DDF_{Ice}) surfaces. PDDs are here applied as in Fausto et al. (2009) to calculate melt volume from mean monthly near-surface air temperatures with monthly standard deviation (σ) of temperatures. The σ data enable accounting for melt in months with average air temperatures below 0°C. The 1958–2008 period is assumed to have equivalent variance as earlier and later periods in the reconstruction. Here, $DDF_{Ice} = 9.5\,mm\,day^{-1}\,°C^{-1}$ and $DDF_{Snow} = 6.6\,mm\,day^{-1}\,°C^{-1}$ are chosen after an iterative procedure comparing the profile of reconstructed surface mass balance versus elevation with that from 1991–2010 observations along the K transect (van de Wal et al. 2012). The values of DDF_{Ice} and DDF_{Snow} are assumed to be constant in time.

Some meltwater is prevented from escaping as runoff from the ice sheet by refreezing or remaining liquid in the porous firn (e.g., Harper et al. 2012). In this study, a simple meltwater refreeze scheme yields residual runoff, requiring only that some fraction of the annual accumulation must melt before runoff occurs. Consistent with K-transect equilibrium line altitude (ELA) variation observations, we adopt a melt-to-accumulation ratio of 1.45, which implies that 45% more melting than accumulation must occur for meltwater to exit the ice sheet at a given 5-km grid cell. This is similar to analogous west Greenland runoff parameterizations that require 50% more melt than accumulation (Colgan et al. 2011a). The melt-to-accumulation ratio is a convenient tuning parameter representing an unknown combination of errors. In the absence of a fully validated physically based snow model, the tuning is assumed to accurately represent the whole ice sheet. Runoff is calculated from all Greenland ice, including the lowest parts of outlet glaciers resolved by the 5-km grid and ice mask of this study. The land–ice–sea mask receives some additional description in Part II and Kargel et al. (2012).

Validation of the surface mass balance data relative to independent observations from the 1991–2010 period

along the K transect (van de Wal et al. 2012) yields a one standard deviation surface mass balance uncertainty of 55% or 53 Gt yr^{-1} for the whole ice sheet ablation area, which has a 1991–2010 average surface mass balance of −96 Gt yr^{-1} or −0.61-m water equivalence. Accumulation area surface mass balance uncertainty from comparison with ice cores yields a 1σ uncertainty of 16% or 90 Gt yr^{-1} in the accumulation area, which has a 1991–2010 average surface mass balance of 616 Gt yr^{-1} or 0.36-m water equivalence. The calculated whole ice sheet 1σ surface mass balance uncertainty is 117 Gt yr^{-1}, with the ice sheet having a 1991–2010 average surface mass balance of 520 Gt yr^{-1} or 0.28-m water equivalence. Runoff uncertainty is derived from lower ablation area K-transect comparisons in which a 0.54-m water equivalence RMSE scales to a whole ice sheet 1σ uncertainty of 27% or 120 Gt yr^{-1}.

Over the full 171-yr surface mass balance reconstruction, increases in both accumulation and surface melting are evident, producing an overall negligible surface mass balance trend. At decadal time scales, however, significant (25% or ~100 Gt yr^{-1}) variations are caused by interdecadal extremes either in accumulation or surface melting. The absolute magnitude of runoff data at the whole ice sheet scale is less than in other recent studies, such as Ettema et al. (2009), which appears to be due to a larger amount of meltwater retention applied by the surface mass balance reconstruction (Part II).

3. Parameterization of whole ice sheet marine ice loss

At the scale of single glaciers, local-scale effects such as bed and fjord wall shape are prone to dominate ice discharge (e.g., Nick et al. 2009). At the scale of a glacier population, however, a distinct pattern in variability of ice discharge may emerge, similar to how glacier populations exhibit distinct trends in area or volume (Bahr et al. 1997), minimizing the effect of strong individual glacier idiosyncrasy (e.g., Howat et al. 2010; Joughin et al. 2010). Using 3-yr smoothing of surface mass balance data, Rignot et al. (2008) parameterize whole ice sheet ice discharge (the same as L_M here) versus surface mass balance anomaly. We adopt the same approach, but also assess L_M as a function of whole ice sheet runoff. The functional form of the semiempirical parameterization is selected by examining polynomial fits between L_M and surface mass balance and runoff of orders 1 through 3. Surface mass balance is examined first, providing an opportunity to discuss the competing effect of net snow accumulation with runoff. A runoff-based L_M parameterization is proposed and accompanied by discussion of relevant physical mechanisms.

a. Marine ice loss versus surface mass balance

The relation between L_M and surface mass balance may be represented by a linear model, especially when L_M estimates from the more uncertain years 1958 and 1964 are excluded (Fig. 1). The resulting implied functional relation is characterized by increasing marine ice loss with decreasing surface mass balance. The model parameterization allows low accumulation to contribute to high L_M through less meltwater retention in the upper ablation area. In the limit where surface mass balance is extremely positive (>550 Gt yr^{-1}), parameterized L_M approaches zero. This may be interpreted as plausible, considering the growth of ice shelves would be expected under an extremely positive surface mass balance conditions. Analogously, seasonal ice shelves have been observed to develop in the winter season, when there is little to no surface melting (Howat et al. 2010). The lack of explicit ice shelf mechanics may overestimate L_M given the effect of ice shelves buttressing–resisting ice flow, as is presumably the case during times of more widespread ice shelf formation. The most likely period of overestimated L_M is during, and immediately after, the Little Ice Age in the 1840–1915 interval.

The 1958 and 1964 outliers in Fig. 1 are due to low surface mass balance. An inspection of individual years in the surface mass balance data in Part II suggests that the relatively low surface mass balance in both years was caused by not only relatively high melt and runoff, but also relatively low accumulation. In contrast, the 1992 outlier is associated with extremely low melt and runoff due to volcanic cooling induced by Mt. Pinatubo (e.g., Abdalati and Steffen 1997; Box 2002). Year 1996 was a high accumulation year (Part I). Year 2005 was a relatively high melt year and 2009 was a relatively low melt year (Part II). Thus, the competing effects of accumulation and runoff are expected to reduce the sensitivity of L_M to SMB. A multiple linear regression with accumulation and runoff taken as independent explanatory factors suggests that runoff explains more than 80% of the variance in L_M while accumulation explains only 15% of the variance in L_M.

To assess the sensitivity of temporal smoothing, Fig. 2 features the linear fit parameters in the regression between surface mass balance and L_M over a range of time scales. Peak (negative) correlation is found at a smoothing interval of 13 years (Fig. 2a), which suggests that the whole ice sheet marine ice loss response to surface mass balance occurs on the decadal time scale. The regression slope at peak correlation (−1.08) indicates a near 1:1 sensitivity between variations in SMB and L_M at the 13-yr time scale (Fig. 2b). The regression constant at peak correlation (1068 Gt yr^{-1}) may be interpreted as the

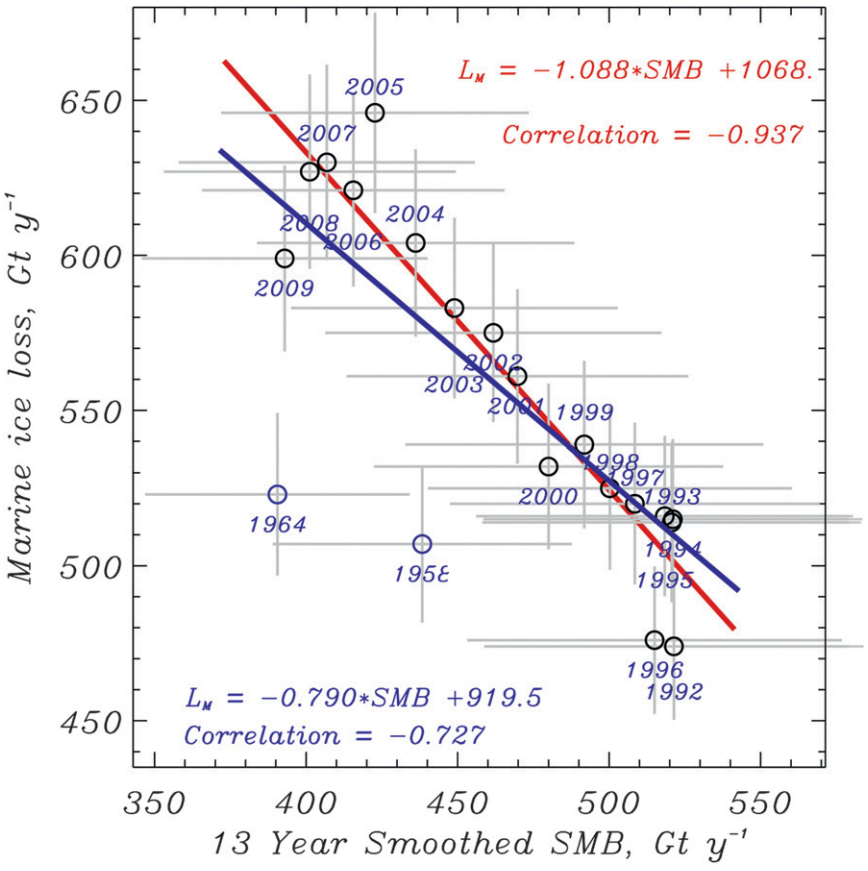

FIG. 1. Empirical fits between smoothed total ice sheet surface mass balance and unsmoothed marine ice loss data after Rignot et al. (2008, 2011). The more uncertain data from 1958 and 1964 (blue circles) are excluded in the red colored fit. Gray lines represent one standard error.

marine ice loss that occurs when surface mass balance is zero (Fig. 2c).

b. *Marine ice loss versus runoff*

Considering runoff as a sole explanatory factor for marine ice loss, a linear correlation sill (Fig. 3a) at 11–13 yr suggests a decadal time scale of peak sensitivity, similar to the SMB regression. In contrast to the SMB regression, however, the regression slope at peak correlation (Fig. 3a) suggests a 1.4 times amplified sensitivity of L_M variability to a given change in runoff. Hence, while the total ice sheet mass budget may be dominated by L_M variability, as suggested by Rignot and Kanagaratnam (2006), runoff may be regarded as ultimately governing L_M. At the limit of zero runoff, the linear regression constant suggests a nonzero L_M (Fig. 3c), which implies a minimum of approximately 100 Gt yr^{-1} ice loss, from background iceberg calving and underwater melting.

At the 13-yr smoothing time scale of best fit, there is minimal difference between the relations of L_M as a function of runoff result from linear and quadratic fits (Fig. 4). A cubic function produces unrealistic extrapolated values beyond the upper and lower limits of reconstructed runoff. Similarly, the quadratic fit suggests unrealistically large L_M values at the low runoff limit. Whether or not 1958 and 1964 estimates for L_M are included does not influence the behavior beyond the observed lower runoff limit. The quadratic fit, however, has lower residuals, including for the post-2004 high runoff and high L_M years. Note that L_M is therefore parameterized as a function of runoff using the quadratic relation when runoff is greater than 270 Gt yr^{-1} and the linear relation when runoff is less than 270 Gt yr^{-1}. This hybrid parameterization acknowledges that a quadratic relation explains observations better than a linear relation, while preventing unrealistic L_M values below the threshold of minimum observed runoff values. The hybrid parameterization for L_M given runoff is chosen over the surface mass balance function for L_M because it has smaller residuals and the 1958 and 1964 estimates are not outliers. The alternative to runoff, meltwater production, was examined but correlated slightly less than runoff data.

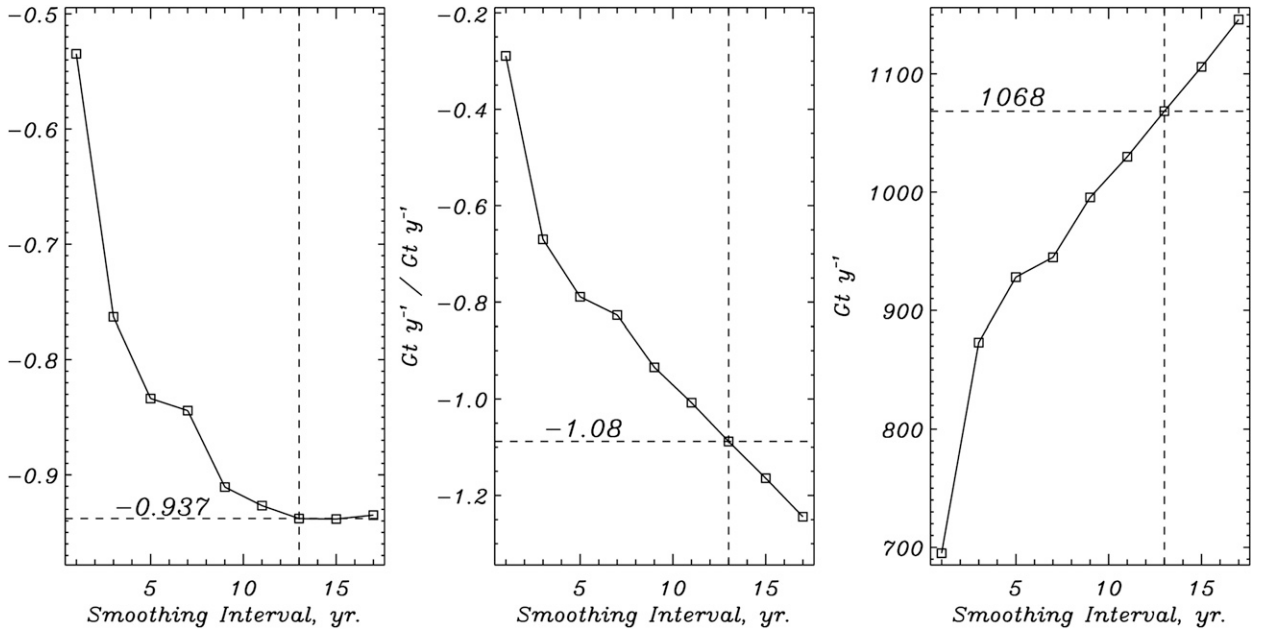

FIG. 2. Fit parameters regression between total ice sheet surface mass balance and marine ice loss data after Rignot et al. (2008, 2011): (left)–(right) correlation, regression slope, and constant. The more uncertain 1958 and 1964 data are not included; although the correlation sill beyond 9-yr smoothing is very similar.

4. Physical basis

Subannual meltwater-induced ice flow acceleration, due to pressurization of the subglacial hydrologic network, has been observed on the inland ice sheet (e.g., Zwally et al. 2002), including a negative feedback following the establishment of an efficient subglacial drainage network (van de Wal et al. 2008; Shepherd et al. 2009; Bartholomew et al. 2010; Sundal et al. 2011). Rignot and Kanagaratnam (2006) find a widespread

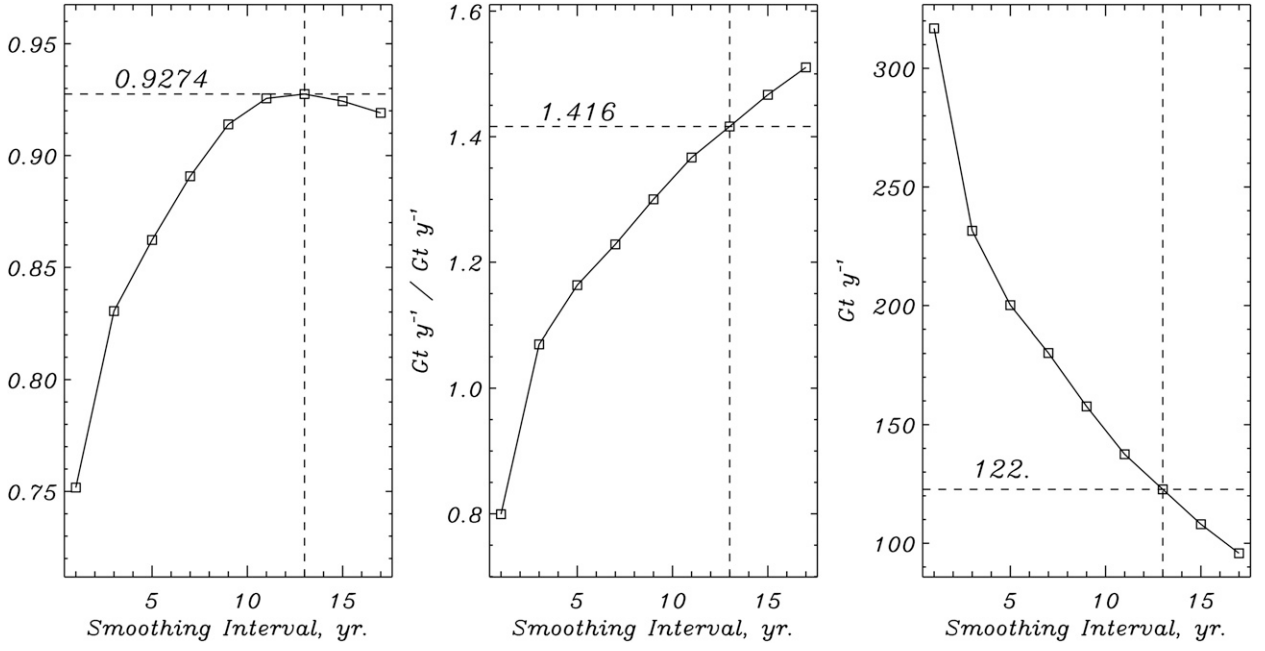

FIG. 3. As in Fig. 2, but for ice sheet runoff.

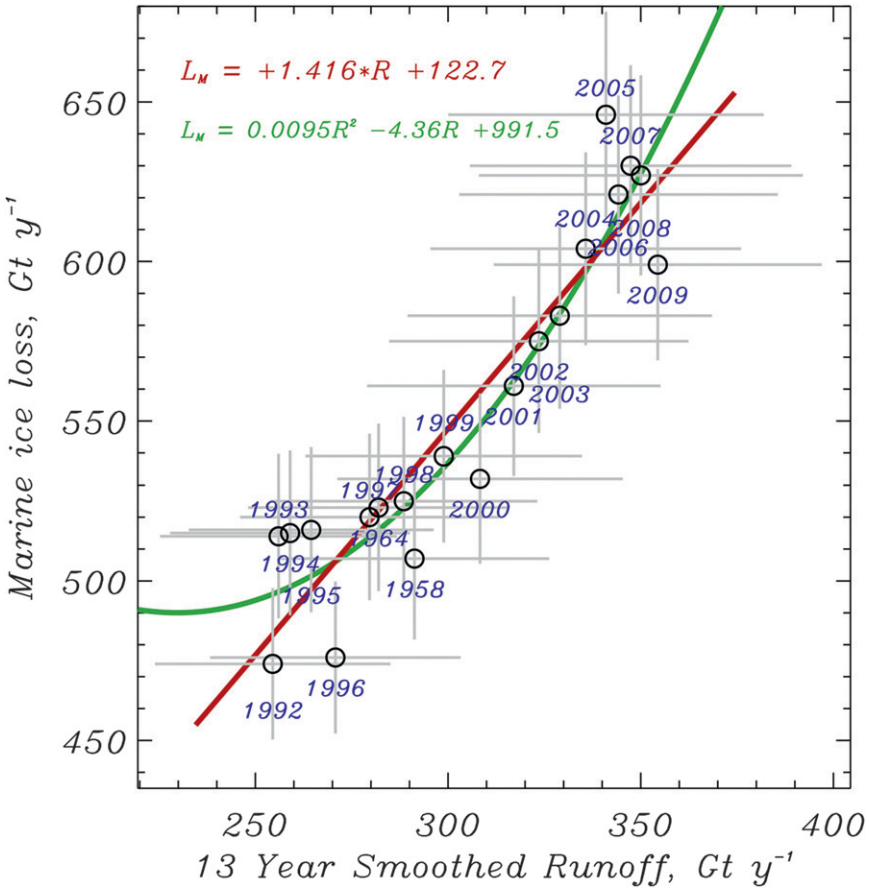

FIG. 4. Comparison of annual total ice sheet marine ice loss and meltwater runoff. Gray lines represent one standard error.

8%–10% increase in summer velocity at Greenland outlet glaciers. While this observed seasonal acceleration occurs on a subannual time scale, we find a decadal time scale of peak L_M sensitivity to both SMB and R (11 yr for SMB and 13 yr for R). As this sensitivity study was not conducted at subannual resolution, it cannot definitively rule out seasonal velocity variations as the driving mechanism for a strong correlation between ice sheet wide runoff and L_M. Indeed, interannual variations in melt season length may underlie the still positive (0.75) correlation at a time interval of 1 year (no smoothing). This assessment does suggest, however, a stronger decadal correlation than an annual correlation between runoff and L_M, which implies that runoff enhances marine ice loss through decadal-scale physical processes, such as decadal changes in basal sliding velocity or temperature-dependent ice viscosity, rather than physical processes that vary on annual or subannual time scales.

Meltwater exits the subglacial environment into the sea, driving the entrainment of seawater, which produces underwater melt rates on the order of meters per day (Motyka et al. 2003; Rignot et al. 2010). This surface meltwater-driven regime of turbulent entrainment of relatively warm and salty seawater, partially forced by runoff ejected from the glacier front, is sufficient to undercut calving fronts, leading to enhanced calving rates (O'Leary and Christoffersen 2013). Iceberg calving (e.g., Benn et al. 2007) directly and immediately reduces the glacier front back-stress resisting ice flow, leading to flow acceleration. Using a numerical ocean circulation model and hydrographic casts, Xu et al. (2012) find that underwater melt rates increase exponentially with subglacial water flux. In addition to wind-driven overturning circulation (Straneo et al. 2010), runoff provides a key mixing mechanism to entrain relatively warm seawater.

While the impact of underwater melting is confirmed on subannual time scales (Rignot et al. 2010), it remains plausible yet unconfirmed that on longer time scales the role of increased runoff rates (e.g., Part II) coupled with global ocean warming (Levitus et al. 2005, 2009) and

warming in Baffin Bay along west Greenland (Zweng and Münchow, 2006) may enhance L_M through enhanced calving. A longer-term physical link between atmospheric (Hansen et al. 2010) and oceanic warming is clear. As time scale increases, the temperature of the air (which directly influences ice sheet runoff) and the ocean temperature covary via their common forcing of the atmosphere and planetary radiation budget. There is good evidence of this effect from analysis of the instrumental meteorological air and sea surface temperature records around the Greenland coast (Hanna et al. 2009). One would thus expect L_M to increase as ocean temperature increases. Indeed, a warm ocean heat pulse has been implicated in destabilizing the Jakobshavn glacier front in the late 1990s (Holland et al. 2008). However, there is also evidence of a negative feedback that may operate between increased runoff and subsequent glacier slowdown via forcing from the ocean in southeast Greenland (Murray et al. 2010).

a. *Feedback between surface melting and crevassing via hydrofracture*

Surface melting delivers water to fill supraglacial depressions, including crevasses. Theoretical calculations by Weertman (1973), van der Veen (1998), and Alley et al. (2005) suggest that a water-filled crevasse can propagate through the entire ice column, due to the inherent density difference between water and ice, forcing water to the subglacial environment. Benn et al. (2007) propose a crevasse criterion based on this process. Nick et al. (2010) made a further modification, suggesting that calving occurs when surface and basal crevasses penetrate the full thickness of the glacier. The proposed calving criterion allows calving losses to be linked to surface melt and therefore climate. The rapid delivery of abundant volumes of water to the subglacial hydrologic system has been observed to result in short-term local velocity accelerations (Das et al. 2008). Crevassed areas absorb more solar radiation, and consequently undergo more ablation, than comparable flat ice areas (Pfeffer and Bretherton 1987). Crevasse extent is transient and has increased near the Jakobshavn glacier, west Greenland, over decadal time scales (Colgan et al. 2011b). Together, these observations suggest that runoff can influence glacier calving rate through increased hydrofracture and crevasse extent, resulting in enhanced meltwater delivery to the bed, and ultimately enhanced basal sliding. Enhanced crevassing also decreases the structural integrity of the ice delivered to the glacier front, enhancing iceberg calving. Under conditions of sufficient runoff, a positive feedback is conceivable among increasing runoff (due to crevasse-enhanced ablation), increasing crevasse hydrofracture (due to enhanced runoff), and tidewater glacier acceleration (resulting in increased crevasse area).

b. *Ice softening is a function of runoff*

A key additional mechanism to produce an ice flow response to surface melting at decadal time scales is ice softening. Once in the englacial or subglacial hydrologic systems, meltwater warms surrounding background ice—primarily by acting as a latent heat source during refreezing (Phillips et al. 2010), and secondarily by acting as a frictional heat source during flow (Nye 1976). As the background ice warms, its effective viscosity decreases, ultimately increasing deformational ice flow velocities (van der Veen et al. 2011; Phillips et al. 2013) and hence calving rates at tidewater glaciers. Ice temperature and velocity take between 5 and 20 years, depending on the characteristic spacing of the englacial network, to reach transient equilibrium with a given surface meltwater forcing (Phillips et al. 2010, 2013). As ice softening due to meltwater is influenced by crevasse extent and cryohydrologic warming, both of which vary over decadal rather than annual time scales, deformational velocity can be expected to influence iceberg calving rate on decadal time scales. Therefore, it is theoretically reasonable to expect a physical basis to underlie the parameterization between L_M and 13-yr smoothed runoff employed in this study (Fig. 4).

5. Error propagation and uncertainty

The impact of uncertainty on parameterized L_M and the total ice sheet mass budget is examined using a Monte Carlo approach. Random Gaussian distributions of runoff uncertainty are propagated through the parameterized L_M time series, as well as the accumulation and runoff time series comprising the total mass budget. Whole ice sheet uncertainty in rates of runoff (σ = 120 Gt yr^{-1} or 27%) and accumulation (σ = 108 Gt yr^{-1} or 12%) are based on the independent in situ data comparison in section 2b. Uncertainty is assumed to increase linearly with time before 1991 when the K-transect surface mass balance data become available. Uncertainty is set to increase to a value of 150% of σ by the year 1840. In years after 1991, a constant uncertainty of 100% σ is assumed.

6. Reconstructed marine ice loss

Parameterized ice sheet total marine ice loss is in the 380–625 Gt yr^{-1} range over the entire 1840–2010 reconstruction, increasing by 50–150 Gt yr^{-1} during periods of elevated surface melting and runoff in the 1920s and since the mid-1990s. Over the full period of

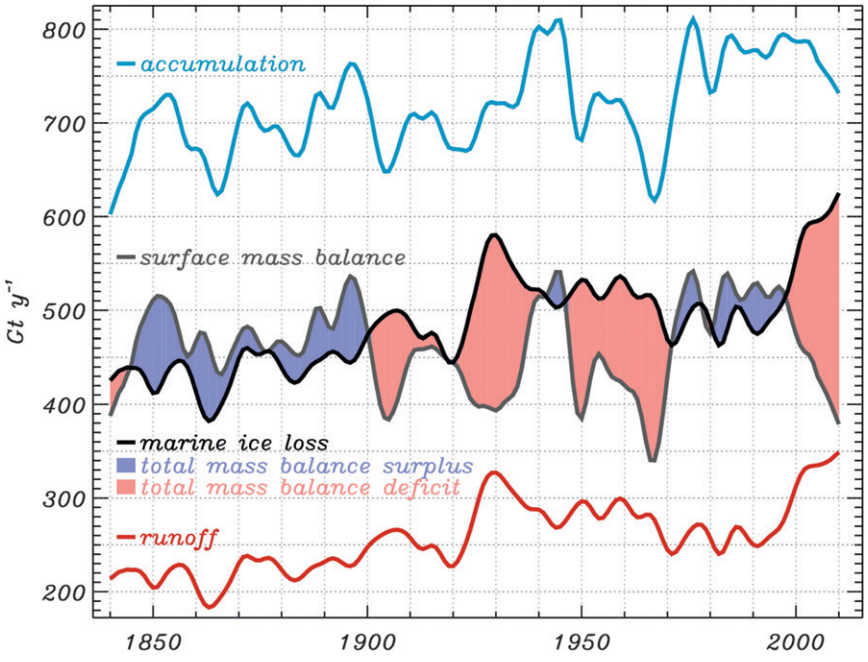

FIG. 5. The 13-yr smoothed reconstructed Greenland ice sheet mass balance subcomponents.

the reconstruction, the parameterization suggests a 49% increase in L_M (or 196 Gt yr^{-1}). In comparison to the hybrid L_M parameterization, the linear L_M parameterization produces a 46% long-term increase. A negative feedback on the long-term L_M increase is a 20% or 122 Gt yr^{-1} accumulation rate increase, which partially offsets a 59% or 186 Gt yr^{-1} increase in meltwater production, which is in turn due to a 51% or 50 Gt yr^{-1} increase in meltwater retention (Part II). Nonetheless, runoff increased 63% or 135 Gt yr^{-1} during the reconstruction period, enhancing the calculated L_M increase.

a. Total ice sheet mass balance

It is possible to close the Greenland ice sheet total mass budget (TMB) by combining the 171 years of accumulation (A) and runoff (R) from Part II with the L_M estimate developed here (Fig. 5):

$$\mathrm{TMB} = A - R - L_M. \quad (1)$$

The mass budget is calculated using the hybrid L_M parameterization [i.e., linear (quadratic) function below (above) $R = 270$ Gt yr^{-1}]. Only year 2010 represents an extrapolation from the observed L_M record to higher runoff values. Since runoff values are smoothed using a 13-yr filter, the results presented here are not highly sensitive the extrapolated 2010 R value. Further, year 2010 is within the time range compared with independent Gravity Recovery and Climate Experiment (GRACE) data.

According to our reconstruction, TMB has been positive for 39% of the 1840–2010 period (see mass balance surplus areas in Fig. 5). The positive decade-scale mass balance phases correspond with periods of low melting and runoff. For example, from ~1970 to ~1985 a positive mass balance phase corresponds to a period of enhanced sulfate cooling (Wild et al. 2009) pronounced along west Greenland (Rozanov et al. 2002; Box et al. 2009). Mass budget surpluses can also be produced by high accumulation years, even occasionally despite relatively high runoff (e.g., 1996).

The reconstructed TMB values are compared 1) with those from the surface mass balance in Part II minus the Rignot et al. (2008, 2011) L_M for 20 samples spanning 1958–2009 and 2) with the independent GRACE data spanning 2003–10 after Wahr et al. (2006) (Fig. 6). We find RMS errors of 31 Gt yr^{-1} for dataset 1 and 69 Gt yr^{-1} in comparison with dataset 2 (Table 1).

b. Sea level contribution

To ensure the most accurate total mass balance reconstruction possible, we scale our reconstructed total mass balance with the independent total mass balance observations of GRACE. This is accomplished by normalizing both the reconstructed TMB and GRACE observations to the 2003–10 period, and applying the resulting regression parameters (slope and constant) to scale the entire TMB reconstruction. Scaling the TMB

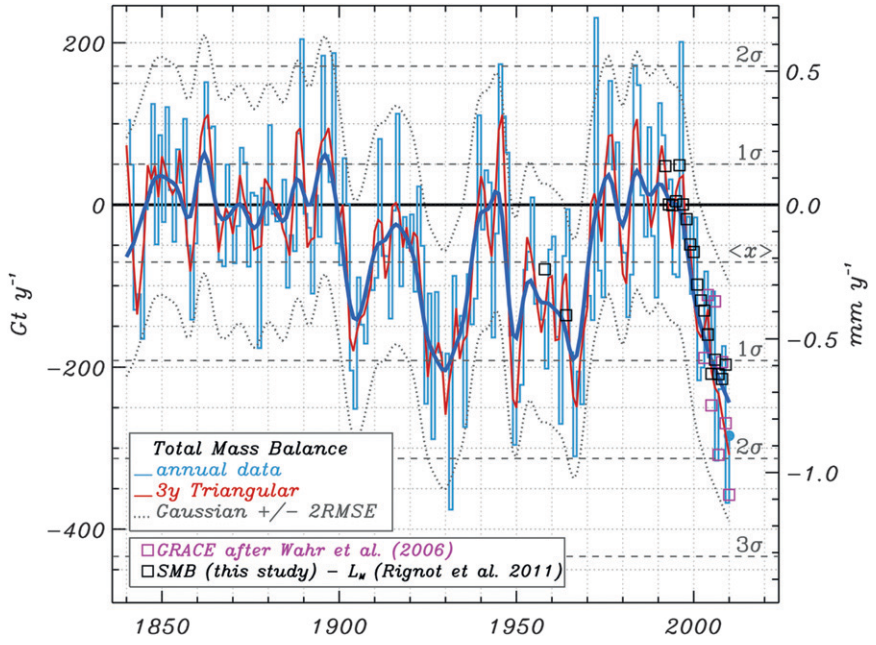

FIG. 6. Whole ice sheet mass balance based on a combination of in situ and simulated climate data reconstruction of surface mass balance (SMB) and parameterized marine ice loss. Results from triangular or Gaussian running average filters are included to illustrate longer-term variations. Gray numbers on the inside of the right ordinate indicate the number of standard deviations from the 1901–2000 baseline period. Total mass balance estimates from other studies are included. The RMSE line is based on residuals after calibration to GRACE data.

reconstruction reduces the RMSE by 16%, to 58 Gt yr^{-1}, and results in a cumulative 1840–2010 sea level contribution of 24.9 mm. By comparison, the cumulative sea level contribution for the reconstruction without the GRACE scaling is 17.1 mm. If dataset 1 were similarly used to scale the reconstruction, the cumulative sea level contribution for the reconstruction is 19.1 mm and the RMSE relative to GRACE increases to 71 Gt yr^{-1}. The parameterization of L_M that we employ, while it can ultimately be expected to have a physical basis, is fundamentally a statistical relation. Thus, the unscaled TMB reconstruction we provide may be regarded as a framework for exploring relative variability in the three major components of TMB to a common climate forcing, rather than the product of a deterministic model. The fully independent GRACE record allows us to scale our TMB reconstruction with recent observations of total ice sheet mass change. While the GRACE direct observation record is only eight years long, it includes a wide variety of total mass changes, from near equilibrium to extreme mass loss years, making the highly transient 2003–2010 period well suited for scaling reconstructed TMB variability. Scaling relatively long reconstructed time series by relatively short observational records has been applied to other geophysical processes, including air temperature (e.g., Mann et al. 1999; von Storch et al. 2004).

The GRACE scaling substantially increases inferred sea level rise contribution over the reconstruction period (from 17 to 25 mm), as the unscaled ice sheet TMB during the 2000s is substantially smaller than observed by GRACE (Fig. 7). In comparison, Zuo and Oerlemans (1997) estimate a cumulative sea level rise contribution from the Greenland ice sheet of 30 mm for the 1865–1990 period. For the same period, our GRACE-calibrated

TABLE 1. Comparison of reconstructed total mass balance with independent GRACE data and the Rignot et al. (2011) data upon which the marine ice loss parameterization was based.

Validation data source	Linear regression coefficient	Linear regression constant	Linear regression correlation	RMSE (Gt yr^{-1})	Average bias (Gt yr^{-1})	Number of years in the comparison
GRACE after Wahr et al. (2006)	1.134	−11.5	0.701	69	37	8
SMB (Part II)–L_M (Rignot et al. 2008, 2011)	0.942	−7.2	0.939	31	−7	20

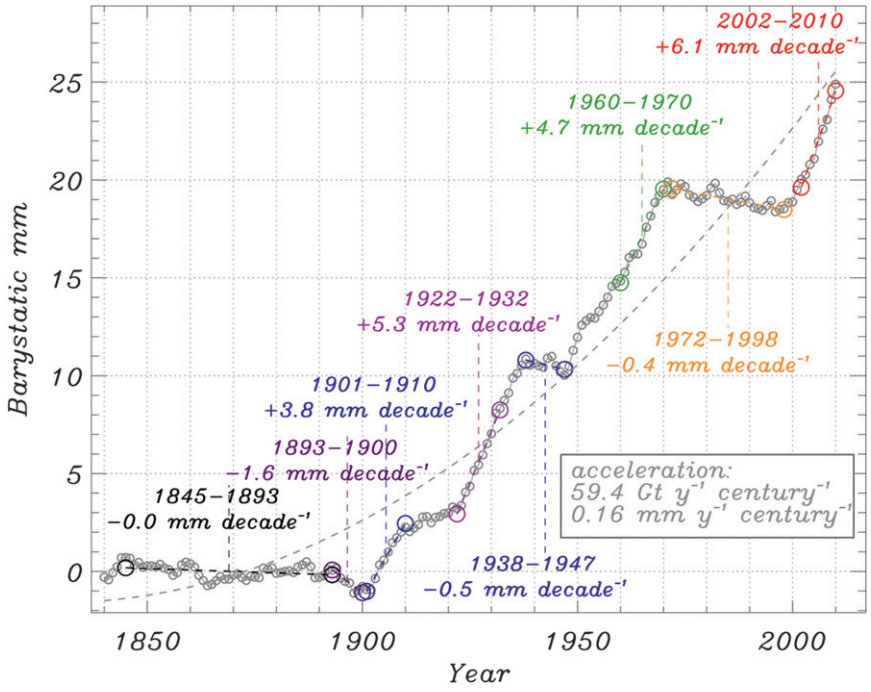

FIG. 7. Greenland ice sheet global eustatic sea level contribution calculated in this study. Rates of change per decade are indicated with time period bounded by colored circles.

reconstruction yields 20 mm. This study does not necessarily disagree with the Zuo and Oerlemans (1997) result; rather, it is within the 1σ error margins of the Monte Carlo simulation ensemble (Fig. 8).

Interdecadal variability in cumulative TMB leads to a positive or negative sign switching from near zero in 1845–93 to various positive or negative phases, peaking in the last 9 yr of the reconstruction characterized by a 6 mm decade^{-1} sea level contribution. A quadratic fit to the cumulative sea level contribution yields apparent acceleration in the ice sheet sea level contribution by 59.4 Gt yr^{-1} century^{-1}. Considering that since 1840 Arctic climate has emerged from the Little Ice Age, in the 1860s Greenland glaciers were near their maximum extent and probably advancing, it is reasonable to expect there to be some acceleration of Greenland sea level contribution since that time, especially amid increasing surface and oceanic temperatures.

7. Conclusions

The combined effects of ice discharge and iceberg calving rates are here grouped into a single mass budget term referred to as "marine ice loss." A marine ice loss parameterization is developed at the scale of the entire Greenland ice sheet where a single relation minimizes the idiosyncratic aspect of individual glacier flow dynamics dominated by local factors. The theory that meltwater runoff ultimately governs marine ice loss abides existing evidence that surface melting and hence runoff enhance marine ice loss through three fundamental processes: 1) increased glacier discharge by ice warming–softening and basal lubrication–sliding; 2) increased calving susceptibility through undercutting glacier front geometry and reducing ice integrity; and 3) increased underwater melting from forcing marine convection. Meltwater warms surrounding ice, primarily by the latent heat released by refreezing and secondarily by turbulent frictional heating, decreasing the effective viscosity of ice and ultimately increasing ice flow and calving rates. Meltwater production is critical for crevasse hydrofracture, which both facilitates the delivery of meltwater to the subglacial environment where it enhances basal sliding and also decreases the structural integrity of ice delivered to the glacier front, ultimately enhancing calving rates. Meltwater runoff ejected at the glacier front has the capacity to entrain seawater, which both enhances underwater ice melting and undercuts glacier front geometry, decreasing structural integrity and back stress against flow. Air and ocean temperatures, both of which directly influence surface and marine melting, demonstrate an increase in covariability with increasing time scale, due to common atmospheric forcing. Generally, a complex and multifaceted positive feedback prevails in the relation between runoff and

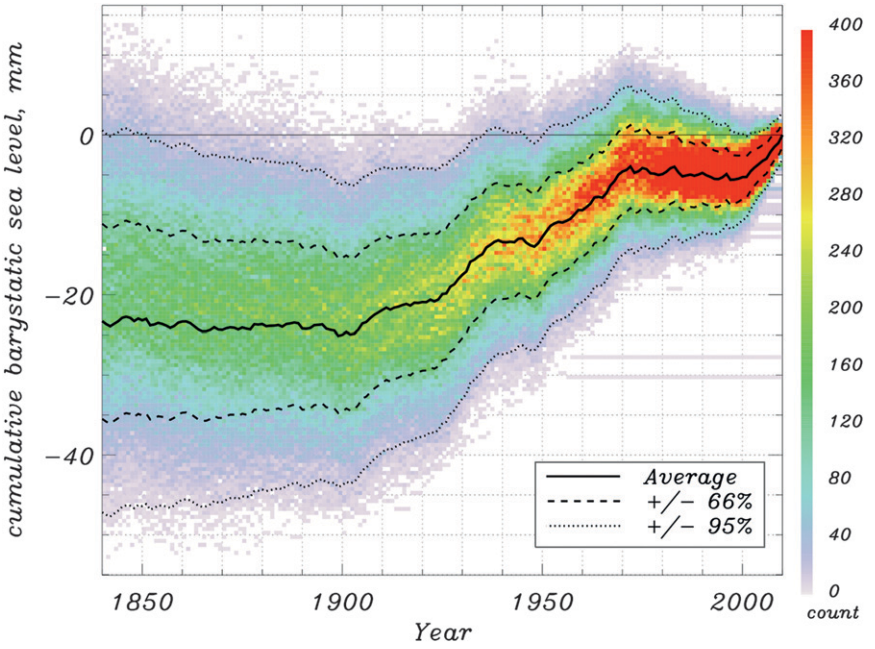

FIG. 8. Greenland ice sheet global sea level contribution with the frequency of 4000 randomly perturbed runoff, accumulation, and marine ice loss values per year and uncertainty increasing linearly backward in time from year 1991 are indicated by colored areas.

marine ice loss, despite negative feedbacks such as the development of efficient subglacial drainage over short time scales or an increase in accumulation rate (and therefore meltwater retention) with increasing near-surface air temperature. Given the numerous links between runoff and marine ice loss, we contend that it is reasonable to parameterize marine ice loss as an empirical first-order function of surface meltwater runoff.

Parameterizing marine ice loss in terms of whole ice sheet meltwater runoff or surface mass balance not only offers a convenient way to close the ice sheet mass budget but also yields physical insight through examination of the empirical fit parameters. For example, the sensitivity of marine ice loss to surface mass balance appears to be linear over the 1840–2010 period, while the sensitivity of marine ice loss to runoff appears to be nonlinear, here approximated by a quadratic function that suggests a factor of 5 increase in marine ice loss for every doubling of meltwater runoff. The competing effect of accumulation simply linearizes the surface mass balance to marine ice loss relation. Multiple regression suggests that runoff explains more than 80% of the variance in ice discharge, while accumulation only explains 15% of the variance. The linear marine ice loss versus runoff regression slope suggests a 42% higher amplitude of marine ice loss for a given change in runoff volume. This implies that variability in runoff ultimately governs much of the marine ice loss variability. In turn, our results suggest that total ice sheet mass balance variability is dominated by surface melting in the period since the end of the Little Ice Age terminating after year 1901.

A runoff Gaussian smoothing interval of 11 or 13 yr produces the highest correlation and smallest residuals in linear and nonlinear fits. This implies a multiyear sensitivity of ice discharge (and iceberg calving) to runoff. Peaks, sills, and asymptotes in the zero-lag correlations are evident, reinforcing the notion of optimal time scales in the statistical functions used to represent physically based relations between ice discharge (and calving rate) and surface mass balance or runoff.

The less certain 1958 and 1964 ice discharge values degrade the correlation between marine ice loss and surface mass balance (Fig. 1). Considering marine ice loss and runoff, the correlation does not change by excluding the more uncertain 1958 and 1964 data (both $\approx$ 0.93). It is clear that in the former case, for surface mass balance versus marine ice loss, anomalous accumulation years in particular produce outliers in an otherwise clear statistical relationship.

The cumulative eustatic sea level contribution scaling to independent GRACE data amounts to 25 $\pm$ 10 mm over the full 171-yr period of our reconstruction. This amount is smaller than previous estimates because our reconstruction includes phases of ice sheet net mass gain (net sea level drawdown) spanning the periods 1893–1900, 1938–47, and 1972–98. Without the GRACE scaling, the 171-yr cumulative sea level contribution amounts to 17 mm. However, it is necessary to make the

GRACE scaling to match reported Greenland mass imbalances derived from those and the Rignot et al. (2011) total mass balance data.

A quadratic fit to the cumulative eustatic sea level contribution yields an apparent acceleration in the ice sheet sea level rise contribution by 27.6 Gt yr^{-1} $century^{-1}$. Considering that since 1840 Arctic climate has emerged from the Little Ice Age when Greenland glaciers were close to their maximum historical extent and probably advancing, it is reasonable to expect an acceleration of Greenland sea level contribution since that time.

Acknowledgments. This work was supported by the Cryospheric Sciences Program of NASA's Earth Science Enterprise Grants NNG04GH70G and NNX07AM82G, The Ohio State University's Climate Water Carbon initiative managed by D. Alsdorf, and the Geologic Survey of Denmark and Greenland (GEUS). Thanks to F. M. Nick, D. H. Bromwich, D. I. Benn, E. Rignot, and M. Pelto for feedback on this manuscript. Three anonymous reviewers are thanked for constructive comments.

REFERENCES

Abdalati, W., and K. Steffen, 1997: The apparent effects of the Mt. Pinatubo eruption on the Greenland ice sheet melt extent. *Geophys. Res. Lett.,* **24,** 1795–1797.

Alley, R. B., T. K. Dupont, B. R. Parizek, and S. Anandakrishnan, 2005: Access of surface meltwater to beds of sub-freezing glaciers: Preliminary insights. *Ann. Glaciol.,* **40,** 8–14.

Bahr, D. B., M. F. Meier, and S. D. Peckham, 1997: The physical basis of glacier volume-area scaling. *J. Geophys. Res.,* **102** (B9), 20 355–20 362.

Bartholomew, I., P. Nienow, D. Mair, A. Hubbard, M. King, and A. Sole, 2010: Seasonal evolution of subglacial drainage and acceleration in a Greenland outlet glacier. *Nat. Geosci.,* **3,** 408–411, doi:10.1038/ngeo863.

Bauer, A., M. Baussart, M. Carbonnell, P. Kasser, P. Perroud, and A. Renaud, 1968: Missions aériennes de reconnaissance au Groenland, 1957–1958. *Medd. Groenl.,* **173** (3), 116 pp.

Benn, D. I., C. R. Warren, and R. H. Mottram, 2007: Calving processes and the dynamics of calving glaciers. *Earth Sci. Rev.,* **82,** 143–179.

Box, J. E., 2002: Survey of Greenland instrumental temperature records: 1873–2001. *Int. J. Climatol.,* **22,** 1829–1847.

——, 2013: Greenland ice sheet mass balance reconstruction. Part II: Surface mass balance (1840–2010). *J. Climate,* **26,** 6974–6989.

——, and Coauthors, 2006: Greenland ice sheet surface mass balance variability (1988–2004) from calibrated Polar MM5 output. *J. Climate,* **19,** 2783–2800.

——, L. Yang, D. H. Bromwich, and L.-S. Bai, 2009: Greenland ice sheet surface air temperature variability: 1840–2007. *J. Climate,* **22,** 4029–4049.

——, and Coauthors, 2013: Greenland ice sheet mass balance reconstruction. Part I: Net snow accumulation (1600–2009). *J. Climate,* **26,** 3919–3934.

Carbonnell, M., and A. Bauer, 1968: Exploitation des couvertures photographiques aeériennes répétées du front des glaciers vélant dans Disko Bugt et Umanak Fjord, juin – juillet 1964. *Medd. Groenl.,* **173** (5), 78 pp.

Church, J. A., and N. J. White, 2011: Sea-level rise from the late 19th to the early 21st century. *Surv. Geophys.,* **32,** 585–602, doi:10.1007/s10712-011-9119-1.

Colgan, W., H. Rajaram, R. Anderson, K. Steffen, T. Phillips, I. Joughin, H. Zwally, and W. Abdalati, 2011a: The annual glaciohydrology cycle in the ablation zone of the Greenland ice sheet: Part 1. Hydrology model. *J. Glaciol.,* **57,** 697–709.

——, K. Steffen, W. McLamb, W. Abdalati, H. Rajaram, R. Motyka, T. Phillips, and R. Anderson, 2011b: An increase in crevasse extent, West Greenland: Hydrologic implications. *Geophys. Res. Lett.,* **38,** L18502, doi:10.1029/2011GL048491.

Das, S. B., I. Joughin, M. D. Behn, I. M. Howat, M. A. King, D. Lizarralde, and M. P. Bhatia, 2008: Fracture propagation to the base of the Greenland ice sheet during supraglacial lake drainage. *Science,* **320,** 778–781.

Ettema, J., M. R. van den Broeke, E. van Meijgaard, W. J. van de Berg, J. L. Bamber, J. E. Box, and R. C. Bales, 2009: Higher surface mass balance of the Greenland ice sheet revealed by high-resolution climate modeling. *Geophys. Res. Lett.,* **36,** L12501, doi:10.1029/2009GL038110.

Fausto, R. S., A. P. Ahlstrøm, D. van As, C. E. Bøggild, and S. J. Johnsen, 2009: A new present-day temperature parameterization for Greenland. *J. Glaciol.,* **55,** 95–105.

Fichefet, T., C. Poncin, H. Goosse, P. Huybrechts, I. Janssens, and H. Le Treut, 2003: Implications of changes in freshwater flux from the Greenland ice sheet for the climate of the 21st century. *Geophys. Res. Lett.,* **30,** 1911, doi:10.1029/2003GL017826.

Hanna, E., and Coauthors, 2008: Increased runoff from melt from the Greenland ice sheet: A response to global warming. *J. Climate,* **21,** 331–341.

——, J. Cappelen, X. Fettweis, P. Huybrechts, A. Luckman, and M. H. Ribergaard, 2009: Hydrologic response of the Greenland ice sheet: The role of oceanographic forcing. *Hydrol. Processes,* **23,** 7–30, doi:10.1002/hyp.7090.

Hansen, J., R. Ruedy, M. Sato, and K. Lo, 2010: Global surface temperature change. *Rev. Geophys.,* **48,** RG4004, doi:10.1029/2010RG000345.

Harper, J., N. Humphrey, W. T. Pfeffer, J. Brown, and X. Fettweis, 2012: Greenland ice-sheet contribution to sea-level rise buffered by meltwater storage in firn. *Nature,* **491,** 240–243, doi:10.1038/nature11566.

Hasholt, B., N. Bobrovitskaya, J. Bogen, J. McNamara, S. H. Mernild, D. Milbourn, and D. E. Walling, 2006: Sediment transport to the Arctic Ocean and adjoining cold oceans. *Nord. Hydrol.,* **37,** 413–432.

Holland, D. M., R. H. Thomas, B. de Young, M. H. Ribergaard, and B. Lyberth, 2008: Acceleration of Jakobshavn Isbræ triggered by warm subsurface ocean waters. *Nat. Geosci.,* **1,** 659–664.

Howat, I. M., J. E. Box, Y. Ahn, A. Herrington, and E. M. McFadden, 2010: Seasonal variability in the dynamics of marine-terminating outlet glaciers in Greenland. *J. Glaciol.,* **56,** 601–613.

Huybrechts, P., J. Gregory, I. Janssens, and M. Wild, 2004: Modelling Antarctic and Greenland volume changes during the 20th and 21st centuries forced by GCM time slice integrations. *Global Planet. Change,* **42,** 83–105.

Joughin, I., S. B. Das, M. A. King, B. E. Smith, I. M. Howat, and T. Moon, 2008: Seasonal speedup along the western flank of the Greenland ice sheet. *Science,* **320,** 781–783.

——, B. Smith, I. M. Howat, T. Scambos, and T. Moon, 2010: Greenland flow variability from ice-sheet-wide velocity mapping. *J. Glaciol.,* **56,** 415–430, doi:10.3189/002214310792447734.

Kargel, J. S., and Coauthors, 2012: Greenland's shrinking ice cover: ''Fast times'' but not that fast. *Cryosphere,* **6,** 533–537, doi:10.5194/tc-6-533-2012.

Levitus, S., J. Antonov, and T. Boyer, 2005: Warming of the World Ocean, 1955–2003. *Geophys. Res. Lett.,* **32,** L02604, doi:10.1029/2004GL021592.

——, ——, ——, R. A. Locarnini, H. E. Garcia, and A. V. Mishonov, 2009: Global ocean heat content 1955–2008 in light of recently revealed instrumentation problems. *Geophys. Res. Lett.,* **36,** L07608, doi:10.1029/2008GL037155.

Mann, M., R. Bradley, and M. Hughes, 1999: Northern Hemisphere temperatures during the past millennium: Inferences, uncertainties, and limitations. *Geophys. Res. Lett.,* **26,** 759–762.

Motyka, R. J., L. Hunter, K. A. Echelmeyer, and C. Conner, 2003: Submarine melting at the terminus of a temperate tidewater glacier, LeConte Glacier, Alaska, U.S.A. *Ann. Glaciol.,* **36,** 57–65.

Murray, T., and Coauthors, 2010: Ocean-regulation hypothesis for glacier dynamics in southeast Greenland and implications for ice-sheet mass changes. *J. Geophys. Res.,* **115,** F03026, doi:10.1029/2009JF001522.

Nick, F. M., A. Veili, I. M. Howat, and I. Joughin, 2009: Large-scale changes in Greenland outlet glacier dynamics triggered at the terminus. *Nat. Geosci.,* **2,** 110–114.

——, C. J. Van der Veen, A. Vieli, and D. I. Benn, 2010: A physically based calving model applied to marine outlet glaciers and implications for the glacier dynamics. *J. Glaciol.,* **56,** 781–794.

Nye, J., 1976: Water flow in glaciers: Jökulhlaups, tunnels and veins. *J. Glaciol.,* **17,** 181–206.

O'Leary, M., and P. Christoffersen, 2013: Calving on tidewater glaciers amplified by submarine frontal melting. *Cryosphere,* **7,** 119–128, doi:10.5194/tc-7-119-2013.

Pfeffer, W. T., and C. Bretherton, 1987: The effect of crevasses on the solar heating of a glacier surface. *IAHS Publ.,* **170,** 191–205.

——, J. T. Harper, and S. O'Neel, 2008: Kinematic constraints on glacier contributions to 21st-century sea-level rise. *Science,* **321,** 1340–1343, doi:10.1126/science.1159099.

Phillips, T., H. Rajaram, and K. Steffen, 2010: Cryohydrologic warming: A potential mechanism for rapid thermal response of ice sheets. *Geophys. Res. Lett.,* **37,** L20503, doi:10.1029/2010GL044397.

——, ——, W. Colgan, K. Steffen, and W. Abdalati, 2013: Evaluation of cryo-hydrologic warming as an explanation for increased ice velocities in the wet snow zone, Sermeq Avannarleq, West Greenland. *J. Geophys. Res.,* doi:10.1002/jgrf.20079, in press.

Rahmstorf, S., and Coauthors, 2005: Thermohaline circulation hysteresis: A model intercomparison. *Geophys. Res. Lett.,* **32,** L23605, doi:10.1029/2005GL023655.

Rignot, E., and P. Kanagaratnam, 2006: Changes in the velocity structure of the Greenland ice sheet. *Science,* **311,** 986–990.

——, J. E. Box, E. Burgess, and E. Hanna, 2008: Mass balance of the Greenland ice sheet from 1958 to 2007. *Geophys. Res. Lett.,* **35,** L20502, doi:10.1029/2008GL035417.

——, M. Koppes, and I. Velicogna, 2010: Rapid submarine melting of the calving faces of West Greenland glaciers. *Nat. Geosci.,* **3,** 187–191, doi:10.1038/ngeo765.

——, I. Velicogna, M. R. van den Broeke, A. Monaghan, and J. Lenaerts, 2011: Acceleration of the contribution of the Greenland and Antarctic ice sheets to sea level rise. *Geophys. Res. Lett.,* **38,** L05503, doi:10.1029/2011GL046583.

Rozanov, E. V., and Coauthors, 2002: Climate/chemistry effects of the Pinatubo volcanic eruption simulated by the UIUC stratosphere/troposphere GCM with interactive photochemistry. *J. Geophys. Res.,* **107,** 4594, doi:10.1029/2001JD000974.

Rysgaard, S., T. Vang, M. Stjernholm, B. Rasmussen, A. Windelin, and S. Kiilsholm, 2003: Physical conditions, carbon transport, and climate change impacts in a northeast Greenland fjord. *Arctic, Antarct. Alp. Res.,* **35,** 301–312.

Shepherd, A., A. Hubbard, P. Nienow, M. King, M. McMillan, and I. Joughin, 2009: Greenland ice sheet motion coupled with daily melting in late summer. *Geophys. Res. Lett.,* **36,** L01501, doi:10.1029/2008GL035758.

Straneo, F., G. Hamilton, D. Sutherland, L. Stearns, F. Davidson, M. Hammill, G. Stenson, and A. Rosing-Asvid, 2010: Rapid circulation of warm subtropical waters in a major glacial fjord off east Greenland. *Nat. Geosci.,* **3,** 182–186, doi:10.1038/ngeo764.

Sundal, A. V., A. Shepherd, P. Nienow, E. Hanna, S. Palmer, and P. Huybrechts, 2011: Melt-induced speed-up of Greenland ice sheet offset by efficient subglacial drainage. *Nature,* **469,** 522–524.

Thomas, R. H., 2004: Force-perturbation analysis of recent thinning and acceleration of Jakobshavn Isbræ, Greenland. *J. Glaciol.,* **50,** 57–66.

van de Wal, R. S. W., W. Boot, M. R. van den Broeke, C. J. P. P. Smeets, C. H. Reijmer, J. J. A. Donker, and J. Oerlemans, 2008: Large and rapid melt-induced velocity changes in the ablation zone of the Greenland ice sheet. *Science,* **321,** 111–113.

——, ——, C. J. P. P. Smeets, H. Snellen, M. R. van den Broeke, and J. Oerlemans, 2012: Twenty-one years of mass balance observations along the K-transect, West Greenland. *Earth Syst. Sci. Data Discuss.,* **5,** 351–363, doi:10.5194/essdd-5-351-2012.

van der Veen, C. J., 1998: Fracture mechanics approach to penetration of surface crevasses on glaciers. *Cold Reg. Sci. Technol.,* **27,** 31–47.

——, J. C. Plummer, and L. A. Stearns, 2011: Controls on the recent speed up of Jakobshavn Isbræ, West Greenland. *J. Glaciol.,* **57,** 770–782, doi:10.3189/002214311797409776.

von Storch, H., E. Zorita, J. Jones, Y. Dimitriev, F. González-Rouco, and S. Tett, 2004: Reconstructing past climate from noisy data. *Science,* **306,** 679–682.

Wahr, J., S. Swenson, and I. Velicogna, 2006: Accuracy of GRACE mass estimates. *Geophys. Res. Lett.,* **33,** L06401, doi:10.1029/2005gl025305.

Weertman, J., 1973: Can a water-filled crevasse reach the bottom surface of a glacier? *IAHS Publ.,* **95,** 139–145.

Wild, M., B. Trüssel, A. Ohmura, C. N. Long, G. König-Langlo, E. G. Dutton, and A. Tsvetkov, 2009: Global dimming and brightening: An update beyond 2000. *J. Geophys. Res.,* **114,** D00D13, doi:10.1029/2008JD011382.

Xu, Y., E. Rignot, D. Menemenlis, and M. Koppes, 2012: Numerical experiments on subaqueous melting of Greenland tidewater glaciers in response to ocean warming and enhanced subglacial runoff. *Ann. Glaciol.,* **53,** 229–234.

Zuo, Z., and J. Oerlemans, 1997: Contribution of glacier melt to sea level rise since AD 1865: A regionally differentiated calculation. *Climate Dyn.,* **13,** 835–845.

Zwally, H. J., W. Abdalati, T. Herring, K. Larson, J. Saba, and K. Steffen, 2002: Surface melt-induced acceleration of Greenland ice sheet flow. *Science,* **297,** 218–222.

Zweng, M. M., and A. Münchow, 2006: Warming and freshening of Baffin Bay, 1916–2003. *J. Geophys. Res.,* **111,** C07016, doi:10.1029/2005JC003093.